α-particle production: Direct and compound contribution in the reaction ⁷Li + ²⁸Si at near-barrier energies

A. Pakou,[1] N. G. Nicolis,[1] K. Rusek,[2] N. Alamanos,[3] G. Doukelis,[4] A. Gillibert,[3] G. Kalyva,[5] M. Kokkoris,[6] A. Lagoyannis,[5] A. Musumarra,[7] C. Papachristodoulou,[1] G. Perdikakis,[5] D. Pierroutsakou,[8] E. C. Pollacco,[3] A. Spyrou,[5] and Ch. Zarkadas[5]

[1]*Department of Physics, The University of Ioannina, GR-45110 Ioannina, Greece*
[2]*Department of Nuclear Reactions, The Andrzej Sołtan Institute for Nuclear Studies, Hoża 69, PL-00-681 Warsaw, Poland*
[3]*DSM/DAPNIA CEA SACLAY, F-91191 Gif-sur-Yvette, France*
[4]*Technical Educational Institute of Athens, GR-12210 Athens, Greece*
[5]*National Research Center, Demokritos, Greece*
[6]*National Technical University of Athens, Athens, Greece*
[7]*Dipartimento di Metodologie Fisiche e Chimiche per l'Ingegneria dell'Universita di Catania, Catania, Italy*
[8]*INFN Sezione di Napoli, I-80125 Napoli, Italy*
(Received 22 July 2004; published 21 June 2005)

The production of α particles in the ⁷Li + ²⁸Si reaction was studied at near-barrier energies. Angular distributions were measured at four energies, namely 9, 10, 11, and 13 MeV. The data were treated in a statistical model and DWBA framework to disentangle the degree of competition between direct and compound channels in the reaction and its energy evolution near the barrier. It was found that whereas the compound mechanism is substantial, *d* transfer and possibly *t* transfer are the dominant mechanism at near-barrier energies. The influence of the reaction channels on the optical potential threshold anomaly is discussed.

I. INTRODUCTION

In the past years, considerable experimental effort has been devoted to elastic scattering and reaction mechanisms (breakup and/or transfer) of weakly bound stable and radioactive nuclei on various targets at near-barrier energies [1–16]. Some of these studies focused on the potential threshold anomaly, whereas others dealt with fusion into a coupled channel framework. As summarized in [5,6], the elastic scattering of the weakly bound nuclei ⁶Li and ⁷Li reveals an anomalous behavior for both the real and the imaginary part of the optical potential in the vicinity of the barrier. This result contrasts with the behavior of the conventional threshold anomaly found in stable nuclei. More explicitly, for ⁶Li the real potential is almost constant with energy, whereas the imaginary part shows an increasing behavior toward lower energies. On the other hand, ⁷Li on heavier targets exhibits the energy-dependent behavior of stable projectiles, by developing a decreasing imaginary potential toward lower energies as the barrier is approached and, in the same energy region, developing a peak for the real part, which however is weaker than the one exhibited by stable projectiles. For the lighter targets, this peak disappears and the potential is again almost constant as for the ⁶Li case. It was suggested that the key to resolving this controversy is obtaining full knowledge of the reaction channels contributing at near-barrier energies. In this context, we report in the present work the measurement of α-production angular distributions of the system ⁷Li + ²⁸Si at near-barrier energies. We also report angular distribution calculations of α production resulting from transfer and fusion into a distorted-wave Born approximation (DWBA) and a Hauser-Feshbach framework, correspondingly, to probe the dominant reaction mechanism via a comparison with the experimental values. As shown by So *et al.* [17] in a semiempirical simultaneous analysis of elastic scattering and fusion data for the system ⁶Li + ²⁰⁸Pb, the fusion channel is responsible for the standard threshold anomaly. This result was obtained by decomposing the polarization potential into a fusion part and a direct part. In this respect, a strong direct channel can wipe out the effect of the anomaly. Therefore, the degree of competition between compound and direct channels is directly related to this effect and thus full knowledge of it is very important.

II. EXPERIMENTAL DETAILS

Our experimental setup was described in detail in a previous work [6] and only a short summary pertinent in this work will be given here. ⁷Li⁺² and ⁷Li⁺³ beams were delivered by the TN11/25 HVEC 5.5-MV Tandem accelerator of the National Research Center of Greece-DEMOKRITOS at four bombarding energies, namely, 9, 10, 11, and 13 MeV. Beam currents were of the order of 30 nA. The beam impinged on a 210 μg/cm² thick, self-supported natural silicon target, tilted by $\pm 45°$ (depending on the detector position) and the reaction products were detected by two telescopes set 24 cm away from the target (the ΔE silicon detector was 10 μm thick, and the E detector was 300 μm thick). The α group was well discriminated by the ΔE-E technique, as can be seen in Fig. 1. Tantalum masks were placed in front of each detector and an angular resolution of 0.7° was obtained. This angular uncertainty was estimated to increase to 1° owing to the beam divergence. The subtending solid angle was 1.2×10^{-4} sr. An overall normalization was obtained at each energy by placing two monitor 300-μm-thick silicon detectors behind the telescopes, 34 cm away from the target, fixed at $\pm 15°$ on a bottom table, and concentric to the top rotating one. The scattering at 15° at the present bombarding energies can be

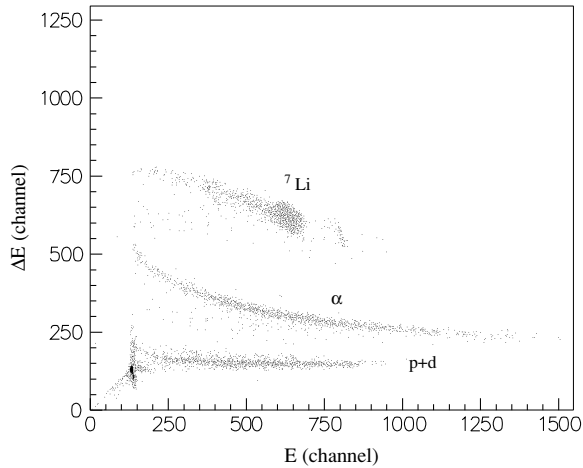FIG. 1. ΔE-E two-dimensional spectrum taken at 13 MeV, $\theta = 75°$ for the system ^{7}Li + ^{28}Si.

considered to be purely Rutherford. A liquid-nitrogen cold trap close to the target holder reduced the target contamination by carbon to a minimum. Likewise, oxygen contamination was made negligible by preserving the targets between our experiments under vacuum. This was confirmed at the end of the runs in a separate Rutherford backscattering experiment, during which the target was tested for oxygen and carbon contaminants and the target thickness was also established. It was found that angular distributions were determined in steps of $2°$ to $10°$ depending on energy in an angular range of $10°$–$140°$. The data were recorded using a PC-controlled acquisition system and were analyzed off-line.

III. ANALYSIS OF THE RESULTS

Energy spectra at $\theta_{lab} = 27°$ for three energies are shown in Fig. 2; the obtained angular distributions are presented in Fig. 3. Both energy spectra and the shape of the distributions can possibly be used to disentangle the various reaction channels involved in the studied process. A possible source of α production could be either a compound or a direct mechanism.

To estimate the compound contribution we have performed calculations with the newly developed Monte Carlo statistical model evaporation code MECO [18]. The code uses optical model transmission coefficients for particle emission and default γ-ray strengths as in the code PACE [19]. Level density parameters are obtained from the compilation of Gilbert and Cameron [20]. The excitation energy dependence and asymptotic high-energy limits of these parameters are given according to the ansartz of Ignatyuk *et al.* [21]. Compound nucleus spin distributions are calculated with transmission coefficients obtained by a one-dimensional barrier penetration model using the Bass nuclear potential [22].

A comparison of compound α-particle yields calculated with MECO and PACE is shown in Table I. As is seen at the lower energies of the present investigation both codes produce the same results. At the highest bombarding energy, MECO produces 20% lower yields than PACE. This difference is mainly
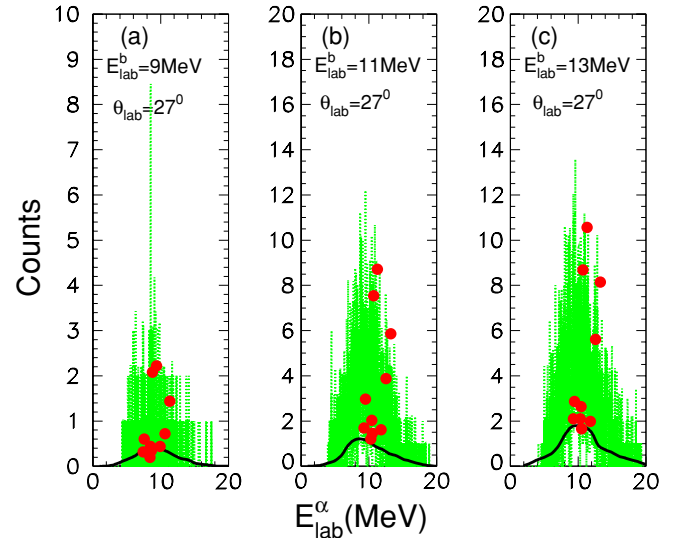

FIG. 2. (Color online) α-particle energy spectra at 9, 11, and 13 MeV (gray part of the spectrum) observed at $27°$ in the laboratory. The solid line represents a simulated α spectrum into a statistical model framework obtained with the code MECO. The filled circles represent a simulated ^{5}He spectrum into a DWBA framework owing to a d-transfer reaction; the α spectrum is expected to be similar. Note that the d-transfer reaction leads to ten discrete low-lying states in ^{30}P. Each filled circle corresponds to one of these states.

due to the use of excitation-energy-dependent level density parameters in MECO. The α-evaporation channels leading to the daughter nuclei ^{27}Al, ^{29}Si, ^{30}Si, and ^{30}P account for 75% of the total fusion cross section. The α-energy spectra, calculated at a laboratory angle of $27°$ with a Monte Carlo simulation via the code MECO, are compared with the data in Fig. 2 at 9, 11, and 13 MeV. The angular distributions resulting from the compound mechanism are presented in Fig. 4 for the same energies. As is seen from the calculations, α particles
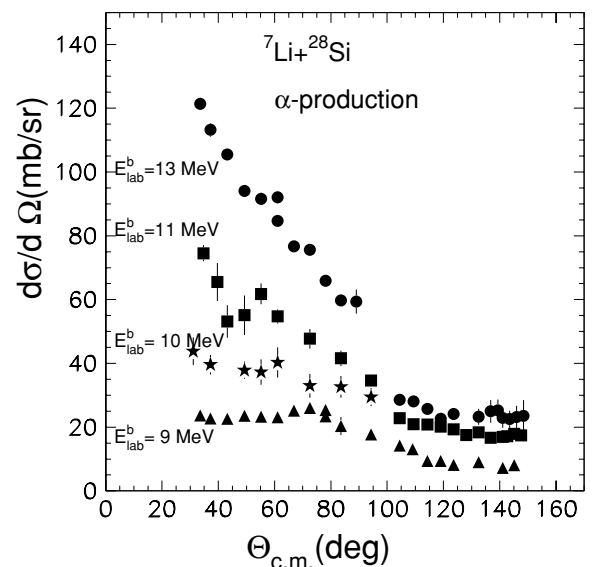

FIG. 3. Measured angular distibutions of the α group in the reaction ^{7}Li + ^{28}Si at the four energies of the present work.

TABLE I. Total α evaporation cross sections obtained by the codes PACE and MECO.

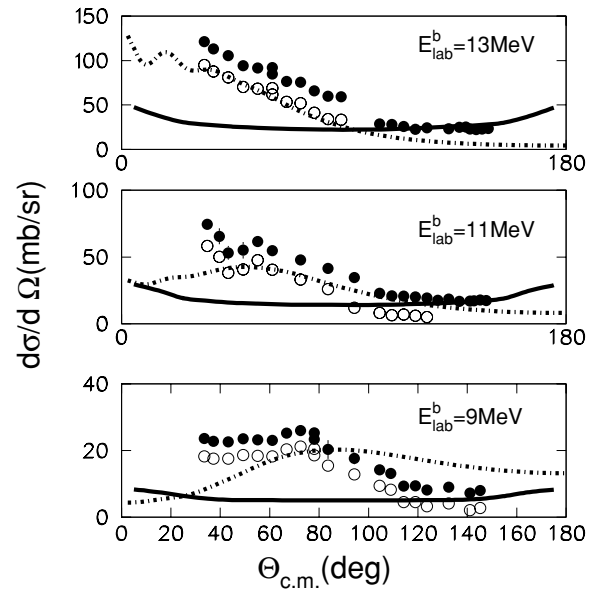| E_{lab} (MeV)	σ(mb)		%Difference
	PACE	MECO	
9.0	75	68	10.3
10.0	151	135	11.9
11.0	236	200	18
13.0	401	320	25

FIG. 4. Angular distributions of the α group in the reaction ^{7}Li + ^{28}Si at 9, 11, and 13 MeV. Data for total α production are designated with filled circles [23]. The dotted-dashed line represents an angular distribution of a d-transfer reaction according to DWBA calculations; the solid line corresponds an α angular distribution resulting from evaporation, obtained with the code MECO. The compound part was subtracted from the data (filled circles) and the resulting "data" representing the direct part are designated with open circles [23]. Since the transfer calculation was in arbitrary units it was scaled to the transfer data. It should be noted that a t-transfer mechanism is not excluded, as is explained in the introduction. The d-transfer calculations follow very well the "data" at 13 MeV, but not at lower energies (e.g., 9 MeV) where the inclusion of t transfer may improve the fit.

are produced with an almost isotropic angular distribution, since they are emitted from a compound nucleus with a very small velocity and angular momentum. It can be noted also that these calculations reproduce adequately well the data at backward angles where the mechanism is assumed to be pure compound. This compatibility gives us the opportunity to disentangle the compound from the direct part of the reaction by subtracting from the experimental cross sections at each angle the calculated compound values. The obtained "new data," which are shown in Fig. 4 with open circles and are tabulated in [23], represent angular distributions of α particles produced via direct processes.

The emission of α particles via direct processes can be attributed to several mechanisms: (a) breakup (^{7}Li $\rightarrow \alpha$+t), (b) d transfer ($Q = +2.2$ MeV), (c) n transfer ($Q = +1.2$ MeV), (d) p transfer ($Q = -7.2$ MeV), and (e) t transfer ($Q = +15.4$ MeV). In this paper we are going to take into account only process (b), that is, d transfer leading to ^{30}P. This nucleus shows many discrete states at low excitation energy and thus process (b) could lead finally to a broad α spectrum. The other processes are excluded for the following reasons. For process (a) breakup Continuum-Discretized Coupled-Channel (CDCC) calculations at 13 Mev for ^{7}Li give a cross section less than 1 mb; however, similar calculations for ^{6}Li give a breakup cross section equal to 16 mb. Provided that preliminary experimental evidence limits the ^{6}Li exclusive breakup to very small values, $\sigma = (4 \pm 6)$ mb [24], which is more or less compatible within two standard deviations with the threrotical value, we conclude that the calculated value of 1 mb can be considered as an upper limit and thus breakup of ^{7}Li on silicon can be considered as negligible. Process (c), that is, n transfer, may result in α production if it leads to ^{6}Li states above the breakup threshold (1.47 MeV). Test calculations for the excitation of the ^{6}Li 3^+resonance (2.18 MeV) generated angular distributions compatible in shape with the data, but not in magnitude (cross sections were smaller by a factor of 30). Furthermore, no sharp peak was observed in our particle spectrum corresponding to transfer to the ^{6}Li ground state. Process (d) is excluded because of the large negative Q value; it could not generate α particles at the range of energies observed in the present experiment. However, because of the very large positive Q value, process (e), that is, t transfer, proceeds to the ground state of ^{31}P with a very small cross section. It could proceed with a substantial cross section to high excitation energies near the breakup threshold of ^{31}P $\rightarrow$ ^{28}Si + t at 15 MeV, but the discrete states in

this region are not known and it would be unwise to make any further speculation in the context of the present work.

Therefore, we will continue with a short description of the DWBA calculations for the d transfer channel. DWBA calculations were performed by means of the computer code FRESCO, version frxp18 [25]. The effective entrance channel optical potential used (^{7}Li + ^{28}Si) was composed of two parts, a bare potential and a Dynamic Polarization Potential (DPP) resulting from breakup (Fig. 5). The bare potential was derived from the cluster-target empirical optical potential by means of cluster-folding method; the DPP potential was generated by the channel coupling in a CDCC calculation, according to the method described by Thompson et $al.$ [26]. Optical model calculations with this effective potential give results very close to full CDCC calculations. The exit channel potential, ^{5}He $+$ ^{30}P, was generated from the empirical n-^{30}P and α-^{30}P optical potential [27], which was folded with the ^{5}He ground-state wave function (cluster-folding method). The geometry of the ^{5}He $+$ d potential was taken as that predicted by Buck and Merchant [28] for α + t. Spectroscopic amplitudes were taken from Nemets et $al.$ [29]; spectroscopic amplitudes for the different states of the final nucleus are from de Meijer et $al.$ [30]. The latter are relative spectroscopic amplitudes to the 7^+ excited state of ^{30}P. For this reason, our results in Fig. 4 were normalized to the "new data," that is, the cross

TABLE II. Total reaction cross sections σ_{tot}, measured previously via elastic scattering [6] (second column). Total α-production cross sections σ_α, presently measured (third column), calculated α cross sections from fusion $\sigma_\alpha{}^f$ (fourth column) and transfer cross sections $\sigma_\alpha{}^t$ (fifth column). The transfer cross sections $\sigma_\alpha{}^t$ were obtained by subtracting the fusion cross section $\sigma_\alpha{}^f$ from the total α cross section σ_α (see text) and may be taken as an upper limit to d- and possibly t-transfer mechanisms. Finally, the sixth column presents the ratio of transfer to fusion.

E_{lab} (MeV)	σ_{tot}(mb)	σ_α (mb)	$\sigma_\alpha{}^f$ (mb)	$\sigma_\alpha{}^t$(mb)	Ratio
9.0	190 ± 58	228 ± 25	68	160 ± 25	2.35 ± 0.37
10.0	413 ± 19	386 ± 45	135	251 ± 45	1.85 ± 0.33
11.0	637 ± 35	476 ± 50	200	276 ± 50	1.38 ± 0.25
13.0	867 ± 39	685 ± 45	320	365 ± 45	1.14 ± 0.14

sections obtained from the data after the compound part was subtracted. As can be seen, the shape of the distributions is well reproduced at least for the forward angles. For the backward angles, calculations fail to reproduce the data at lower energies, especially at 9 MeV. An implementation in the future of the t-transfer process may improve the fit. Additionally, simulated α-energy spectra according to the d transfer are presented in Fig. 2 and these also show good consistency with the data.

IV. DISCUSSION

Taking into account energy spectra and angular distributions into both an evaporation and a direct framework, we can conclude that α production for the system ^{7}Li + ^{28}Si originates mainly via compound and d-transfer processes without excluding t-transfer. Therefore, we can extract the direct part of the reactions consisting certainly of d and possibly of t-transfer process mechanisms by subtracting from total α-production cross sections the calculated fusion ones. The results are shown in Table II and are also compared with total reaction cross sections obtained previously via elastic scattering [6]. Ratios of α cross sections resulting from transfer (d transfer and possibly t transfer) over fusion are also shown in the same table and in Fig. 6. As can be seen, the contribution of the compound mechanism is substantial but drops off rapidly toward lower energies. Transfer dominates near the barrier and therefore possibly leads to a net constant effect for the energy dependence of the potential in this energy region assuming according to [17] that fusion is responsible for the potential anomaly. Preliminary Coupled Reaction Channel Calculations (CRC) were performed and the DPP potential resulting from transfer was derived. The influence of this polarizing potential on the effective potential (bare plus breakup) could be dramatic as can be seen from Fig. 5, where both potentials are compared. Full coupled reaction channel calculations, including this DPP potential resulting from transfer, will be a real challenge for the near future. Since this potential is energy dependent it may well smooth out the attractive polarization potential resulting from the anomaly, as we have suggested previously [5–7].

Another issue we would like to stress here is that the presently measured α-production cross sections as a function of energy follow well the universal curve obtained previously by ^{6}Li α-production cross sections from various targets [7]
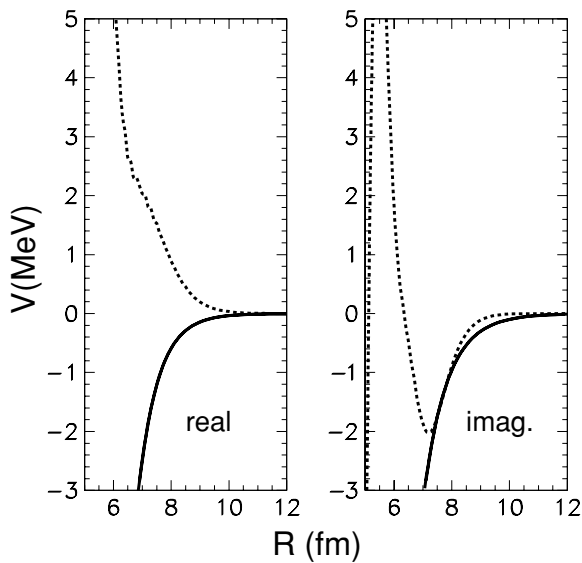

FIG. 5. Effective (bare + breakup) potential designated with the solid line and polarization potentials resulting from transfer designated with the dashed line, for ^{7}Li + ^{28}Si at 13 MeV.
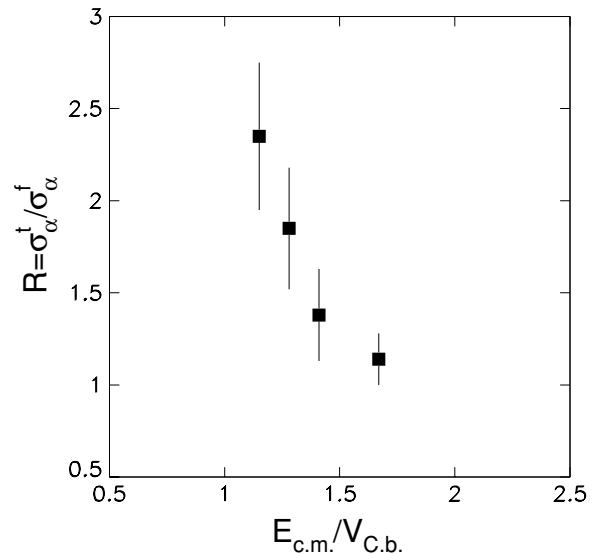

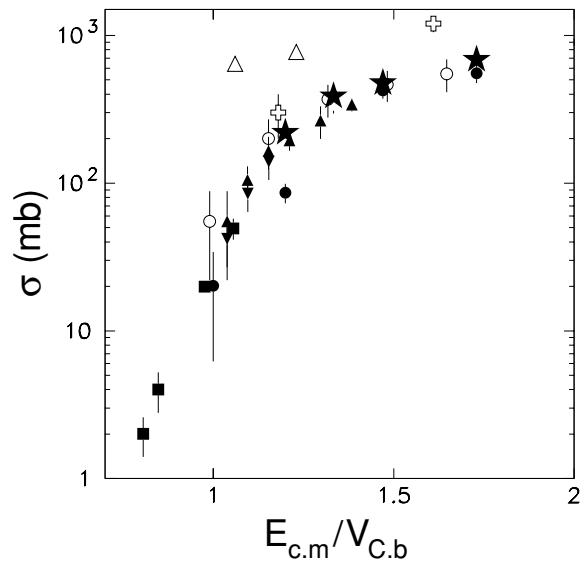FIG. 6. Energy evolution of the competition between transfer and compound processes for α production of the reaction ^{7}Li + ^{28}Si.

FIG. 7. α production cross sections over energy divided by the Coulomb barrier for ^{6}Li on various targets (Si, Ni, Sn, and Pb; see Ref. [7]). Present measurements of ^{7}Li on Si are designated with the big stars and seem to reproduce well the universal behavior of the ^{6}Li α production. α production for ^{6}He on ^{209}Bi [9] and ^{64}Zn [8] is designated with open triangles and open crosses, respectively.

(see Fig. 7). The fact that different mechanisms contribute to the α production in each case but the total α cross sections follow the same energy trend seems initially contradictory. However, this may underline the cluster structure of both weakly bound nuclei to α and other particles (t, d). Similar behavior is exhibited by the weakly bound nucleus ^{6}He on ^{209}Bi and ^{64}Zn [8,9], but in this case the α cross sections diverse from those of ^{6,7}Li by almost an order of magnitude.

V. SUMMARY AND CONCLUSIONS

α-production angular distributions were measured at four near-barrier energies for the system ^{7}Li + ^{28}Si. The angular distributions and the energy spectra were treated in a statistical model and DWBA framework to obtain information on the reaction mechanisms and to disentangle the direct and compound channels in the vicinity of the barrier. It was found that, although the contribution of the compound channel is substantial, the dominant mechanism is the direct one and in fact it consists of a d-transfer process without excluding t-transfer. In this context, apart from the α-production cross sections measured at four energies, transfer cross sections, which provide limit of d and t transfer, were determined by subtracting calculated evaporation cross sections from the α-production data. Ratios between fusion and direct cross sections gave the energy evolution of the competition between the two mechanisms and revealed that transfer becomes very strong at near-barrier energies. Therefore it may smooth out the conventional threshold anomaly. Further comprehensive CRC calculations including d and t transfer are necessary to fully disentangle this very interesting issue.

[1] N. Keeley *et al.*, Nucl. Phys. **A571**, 326 (1994).
[2] A. M. M. Maciel *et al.*, Phys. Rev. C **59**, 2103 (1999).
[3] G. R. Kelly *et al.*, Phys. Rev. C **63**, 024601 (2000).
[4] K. O. Pfeiffer, E. Speth, and K. Bethge, Nucl. Phys. **A206**, 545 (1973).
[5] A. Pakou *et al.*, Phys. Lett. **B556**, 21 (2003).
[6] A. Pakou *et al.*, Phys. Rev. C **69**, 054602 (2004).
[7] A. Pakou *et al.*, Phys. Rev. Lett. **90**, 202701 (2003).
[8] A. Di Pietro *et al.*, Phys. Rev. C **69**, 044613 (2004).
[9] E. F. Aguilera *et al.*, Phys. Rev. Lett. **84**, 5058 (2000).
[10] E. F. Aguilera *et al.*, Phys. Rev. C **63**, 061603(R) (2001).
[11] C. Signorini *et al.*, Phys. Rev. C **61**, 061603(R) (2000).
[12] C. Signorini *et al.*, Phys. Rev. C **67**, 044607 (2003).
[13] N. Keeley and K. Rusek, Phys. Lett. **B427**, 1 (1998).
[14] N. Keeley, K. W. Kemper, and K. Rusek, Phys. Rev. C **66**, 044605 (2002).
[15] N. Keeley and K. Rusek, Phys. Rev. C **56**, 3421 (1997).
[16] J. J. Kolata, Eur. Phys. J. **A13**, 117 (2002).
[17] W. Y. So, S. W. Hong, B. T. Kim, and T. Udagawa, Phys. Rev. C **69**, 064606 (2004).
[18] N. G. Nicolis, to be published.
[19] A. Gavron, Phys. Rev. C **21**, 230 (1980).
[20] A. Gilbert and A. G. W Cameron, Can. J. Phys. **43**, 1446 (1965).
[21] A. V. Ignatyuk, G. N. Smirenkin, and A. S. Tishin, Sov. J. Nucl. Phys. **21**, 255 (1975).
[22] R. Bass, Phys. Rev. Lett. **39**, 265 (1977).
[23] See EPAPS Document No. E-PRVCAN-71-389506 for angular distributions and cross sections for the reaction ^{7}Li + ^{28}Si at different energies. A direct link to this document may be found in the online article's HTML reference section. The document may also be reached via the EPAPS homepage (http://www.aip.org/pubservs/epaps.html) or from ftp.aip.org in the directory/epaps/. See the EPAPS homepage for more information.
[24] A. Pakou *et al.*, to be published and contribution to the 14th Symposium of the Hellenic Nuclear Physics Society, Athens, May 27–28, 2004.
[25] I. J. Thompson, Comput. Phys. Rep. **7**, 167 (1988).
[26] I. J. Thompson *et al.*, Nucl. Phys. **A505**, 84 (1989).
[27] W. Wuhr *et al.*, Zeit. fur Phys. A **269**, 365 (1974).
[28] B. Buck and A. Merchant, J. Phys. G **14**, l211 (1988).
[29] O. F. Nemets *et al.*, *Nuclear Clusters in Atomic Nuclei and Many-Nucleon Transfer Reactions* (Ukrainian Academy of Science, Institute for Nuclear Research, Kiev, 1988).
[30] R. J. de Meijer *et al.*, Nucl. Phys. **A386**, 200 (1982).